Supplemental Material can be found at:
http://www.jbc.org/content/suppl/2011/08/31/M111.265900.DC1.html

THE JOURNAL OF BIOLOGICAL CHEMISTRY VOL. 286, NO. 42, pp. 36888–36897, October 21, 2011
© 2011 by The American Society for Biochemistry and Molecular Biology, Inc. Printed in the U.S.A.

Ligand-receptor Interaction between Triterpenoids and the 11β-Hydroxysteroid dehydrogenase type 2 (11βHSD2) Enzyme Predicts Their Toxic Effects against Tumorigenic *r/m* HM-SFME-1 Cells*[S]

Received for publication, May 28, 2011, and in revised form, August 31, 2011 Published, JBC Papers in Press, August 31, 2011, DOI 10.1074/jbc.M111.265900

Hideaki Yamaguchi[‡1], Tao Yu[§], Toshiro Noshita[¶], Yumi Kidachi[‖], Katsuyoshi Kamiie[‖], Kenji Yoshida[‡], Tatsuo Akitaya[‡], Hironori Umetsu[**], and Kazuo Ryoyama[‖]

From the [‡]Department of Pharmacy, Faculty of Pharmacy, Meijo University, 150 Yagotoyama, Tenpaku, Nagoya 468-8503, Japan, the [§]Graduate School of Medicine, Department of Functional Diagnostic Science, Osaka University, 1-7 Yamadaoka, Suita, Osaka 565-0871, Japan, the [¶]Department of Life Sciences, Faculty of Life and Environmental Sciences, Prefectural University of Hiroshima, 562 Nanatsuka, Shobara 727-0023, Japan, the [‖]Department of Pharmacy, Faculty of Pharmacy, Aomori University, 2-3-1 Kobata, Aomori 030-0943, Japan, and the [**]Laboratory of Food Chemistry, Department of Life Sciences, Junior College, Gifu Shotoku Gakuen University, 1-38 Nakauzura, Gifu 055-8288, Japan

The present study deals with *in silico* prediction and *in vitro* evaluation of the selective cytotoxic effects of triterpenoids on tumorigenic human c-Ha-*ras* and mouse c-*myc* cotransfected highly metastatic serum-free mouse embryo-1 (*r*/*m* HM-SFME-1) cells. Ligand fitting of five different triterpenoids to 11β-hydroxysteroid dehydrogenase type 2 (11βHSD2) was analyzed with a molecular modeling method, and glycyrrhetinic acid (GA) was the best-fitted triterpenoid to the ligand binding site in 11βHSD2. Analysis of antiproliferative effects revealed that GA, oleanolic acid, and ursolic acid had selective toxicity against the tumor cells and that GA was the most potent triterpenoid in its selectivity. The toxic activity of the tested triterpenoids against the tumor cells showed good correlations with the partition coefficient (logP) and polar surface area values. Time-lapse microscopy, fluorescence staining, and confocal laser scanning microscopic observation revealed that GA induced morphologic changes typical of apoptosis such as cell shrinkage and blebbing and also disrupted the cytoskeletal proteins. Furthermore, GA exhibited a strong inhibitory effect on 11βHSD2 activity in the tumor cells. Our current results suggest that analysis of the ligand-receptor interaction between triterpenoids and 11βHSD2 can be utilized to predict their antitumor effects and that GA can be used as a possible chemopreventive and therapeutic antitumor agent. To the best of our knowledge, this is the first report on *in silico* prediction of the toxic effects of triterpenoids on tumor cells by 11βHSD2 inhibition.

Triterpenoids, which are biosynthesized in plants by cyclization of squalene, are widely distributed throughout the vegetable kingdom, utilized in many food products and the major components of medicinal plants used in Asian countries (1). There is a growing interest in elucidating the biological and pharmacological roles of triterpenoids in analgesic, anti-inflammatory, anti-tumor, hepatoprotective, and immunomodulatory effects (1), and we have been focusing our attention on certain triterpenoids as multifunctional agents for the prevention and treatment of cancer. Recently, we found that ursolic acid (UA)[2] from apples was selectively toxic to tumorigenic human c-Ha-*ras* and mouse c-*myc* cotransfected highly metastatic serum-free mouse embryo-1 (*r*/*m* HM-SFME-1) cells (2). We further found that glycyrrhetinic acid (GA), a licorice component, was not only selectively toxic to the tumor cells but also more potent than some clinically available antitumor agents in its selectivity (3).

SFME cells, which were established by Loo *et al.* (4), were originally derived from a 16-day-old whole Balb/c mouse embryo and are maintained in a serum-free culture medium. These cells do not undergo growth crisis, maintain their diploid karyotype for extended passages, and are non-tumorigenic *in vivo*. Consequently, they are non-transformed, behave as primary cultures, have a finite lifespan, and display the characteristics of the CNS progenitor cells (5, 6). Another SFME-derived cell line is the *r*/*m* HM-SFME-1 cell line (7). Although SFME cells are non-tumorigenic *in vivo* and require EGF for their survival, growth, and proliferation (5, 6), *r*/*m* HM-SFME-1 cells are tumorigenic and do not require any growth factors such as EGF (8). Analyzing the characteristics and behaviors of normal and tumorigenic SFME cells could be of great importance in the field of toxicological studies for cancer prevention and therapy because they are of the same lineage and simple comparisons of these cells may contribute to our understanding of the behavioral

* This work was supported in part by a grant-in-aid from the Promotion and Mutual Aid Corporation for Private Schools of Japan.
[S] The on-line version of this article (available at http://www.jbc.org) contains supplemental Movies S1 and S2.
[1] To whom correspondence should be addressed: Dept. of Pharmacy, Faculty of Pharmacy, Meijo University, 150 Yagotoyama, Tenpaku, Nagoya 468-8503, Japan. Fax: 81-52-834-8090; E-mail: hyamagu@meijo-u.ac.jp.

[2] The abbreviations used are: UA, ursolic acid; AA, α-amyrin; BA, β-amyrin; CORT, corticosterone; GA, glycyrrhetinic acid; LBS, ligand binding site(s); OA, oleanolic acid; PSA, polar surface area; SFME, serum-free mouse embryo; 11βHSD2, 11β-hydroxysteroid dehydrogenase type 2; *r/m* HM-SFME-1, human c-Ha-*ras* and mouse c-*myc* cotransfected highly metastatic serum-free mouse embryo-1.

Downloaded from www.jbc.org at MEIJO UNIVERSITY, on October 25, 2011

differences between normal and tumor cells in the CNS in their responses to anti-tumor agents.

11β-Hydroxysteroid dehydrogenase type 2 (11βHSD2) requires NAD^+, shows dehydrogenase activity for endogenous glucocorticoids such as corticosterone (CORT; 9–11), and has been reported to be associated most notably with pituitary adenomas in the CNS (12), but also with colonic adenomas (13) and breast (14, 15) and colorectal (16) cancers. The underlying explanation for the aberrant 11βHSD2 expression is uncertain, but it has been postulated to control glucocorticoid regulation of cellular proliferation (17). Results from *in vitro* studies using malignant transformed cell lines demonstrated the anti-proliferative actions of glucocorticoids. Therefore, the local inactivation of glucocorticoids such as CORT by 11βHSD2 could be an important oncogenic process promoting cellular proliferation (18). Furthermore, 11βHSD2 inhibition by GA prevented colon cancer without triggering adverse side effects in the cardiovascular system (13). GA also had adverse effects on the proliferation of pituitary adenomas (19), and 11βHSD2 inhibition induced apoptosis of corticotroph tumor cells (12). Taken together, these reports suggest that 11βHSD2 inhibition can be utilized as a potential therapeutic option in controlling cancer. Thus, prediction of the toxic effects of drugs on tumors can be achieved by investigating 11βHSD2 inhibition *in silico* and also *in vitro* in tumorigenic *r*/*m* HM-SFME-1 cells.

In the present study, in light of our previously reported selective toxicity of GA and UA against the tumor cells, *in silico* prediction and *in vitro* evaluation of the anti-tumor effects of triterpenoids were investigated. Ligand fitting of five triterpenoids to 11βHSD2 was analyzed with a molecular modeling method to predict their cytotoxic effects. Normal SFME and tumorigenic *r*/*m* HM-SFME-1 cells were treated with the triterpenoids to investigate their efficacy as tumor cell-selective toxic agents. Subsequently, the half-maximal inhibitory concentration (IC_{50}) values of the tested triterpenoids for the normal and tumor cells were analyzed with the partition coefficient between 1-octanol and aqueous phases (logP) and the polar surface area (PSA) values to examine whether there were correlations between them. Furthermore, the tumor cells were exposed to GA, which was the most potent triterpenoid in its selective toxicity, and time-lapse microscopy, fluorescence staining, and confocal laser scanning microscopic observation were adopted to analyze the morphologic and cytoskeletal changes. Furthermore, the effects of GA on CORT levels were analyzed to assess the inhibition of 11βHSD2 enzyme activity by GA.

EXPERIMENTAL PROCEDURES

Materials—α-Amyrin (AA) and β-amyrin (BA) were obtained from Funakoshi Co. Ltd. (Tokyo, Japan). GA, oleanolic acid (OA), and UA were from Wako Pure Chemical Industries, Ltd. (Osaka, Japan), Sigma, and Tokyo Chemical Industry Co. Ltd. (Tokyo, Japan), respectively.

In Silico Ligand-Receptor Interaction between Triterpenoids and 11βHSD2—The binding site selection and exploration for 11βHSD2 were carried out as reported previously (20). In brief, 11βHSD1 (Protein Data Bank code 3HFG) was selected as a template for the structure modeling of 11βHSD2 (NCBI reference sequence NM_008289.2) because of its good crystal structure resolution (2.3 Å) and because its information was the latest (from 2009) among the reported 11βHSD1 models. For the construction of the 11βHSD2 model, 100 independent models of the target protein were built using a Boltzmann-weighted randomized modeling procedure in the Molecular Operating Environment 2009.10 (Chemical Computing Group, Inc., Montreal, Canada), which was adapted from reports by Levitt (21) and Fechteler *et al.* (22). The intermediate models were evaluated by a residue packing quality function, which is sensitive to the degrees to which non-polar side chain groups are buried, and hydrogen bonding opportunities are satisfied. The 11βHSD2 model with the best packing quality function and full energy minimization was selected for further analyses. The secondary structures of the 11βHSD2 model exhibited a central six-stranded all-parallel β-sheet sandwich-like structure, flanked on both sides by three helices, which are in agreement with the 11βHSD1 model. Hydrophobic or hydrophilic α-spheres, which were created by the Site Finder module of Molecular Operating Environment 2009.10, were utilized to define potential ligand binding sites (LBS).

The analysis of the ligand-receptor interaction between the ligands (CORT, PubChem CID 5753; AA, PubChem CID 73170; BA, PubChem CID 5318287; GA, PubChem CID 10114; OA, PubChem CID 10494; and UA, PubChem CID 64945) and the 11βHSD2 model was performed with the α-sphere and excluded volume-based ligand-protein docking (ASE-Dock) module of Molecular Operating Environment 2009.10 (23). In the ASE-Dock module, ligand atoms have α-spheres within 1 Å. Based on this property, concave models were created, and ligand atoms from a large number of conformations were generated by superimposition with these points can be evaluated and scored by the maximum overlap with the α-spheres and minimum overlap with the receptor atoms. The ligand fitting scores and ASE scores are then obtained (24). The scoring function used by the ASE-Dock module is based on ligand-receptor interaction energies and the score is expressed as a U_{total} value. The ligand conformations were subjected to energy minimization using the MMF94S force field (25), and 500 conformations were generated using the default systematic search parameters. Five thousand poses per conformation were randomly placed onto the α-spheres located within the LBS in 11βHSD2. From the resulting 500,000 poses, the 200 poses with the lowest U_{total} values were selected for further optimization with the MMF94S force field. During the refinement step, the ligands were free to move within the binding pocket.

Cell Lines and Cell Culture—SFME cells were a gift from Dr. S. Shirahata (Kyushu University, Fukuoka, Japan) and *r*/*m* HM-SFME-1 cells were taken from our cell stocks (7). The basal nutrient medium was a 1:1 mixture of Dulbecco's Modified Eagle's medium and nutrient mixture F-12 Ham (Dulbecco's Modified Eagle's medium/F-12) (26, 27) and supplemented with sodium bicarbonate, sodium selenite, and gentamicin sulfate. Cells were maintained in Dulbecco's Modified Eagle's medium/F-12 supplemented with insulin, transferrin and EGF in 60-mm diameter dishes precoated with bovine

Downloaded from www.jbc.org at MEIJO UNIVERSITY, on October 25, 2011

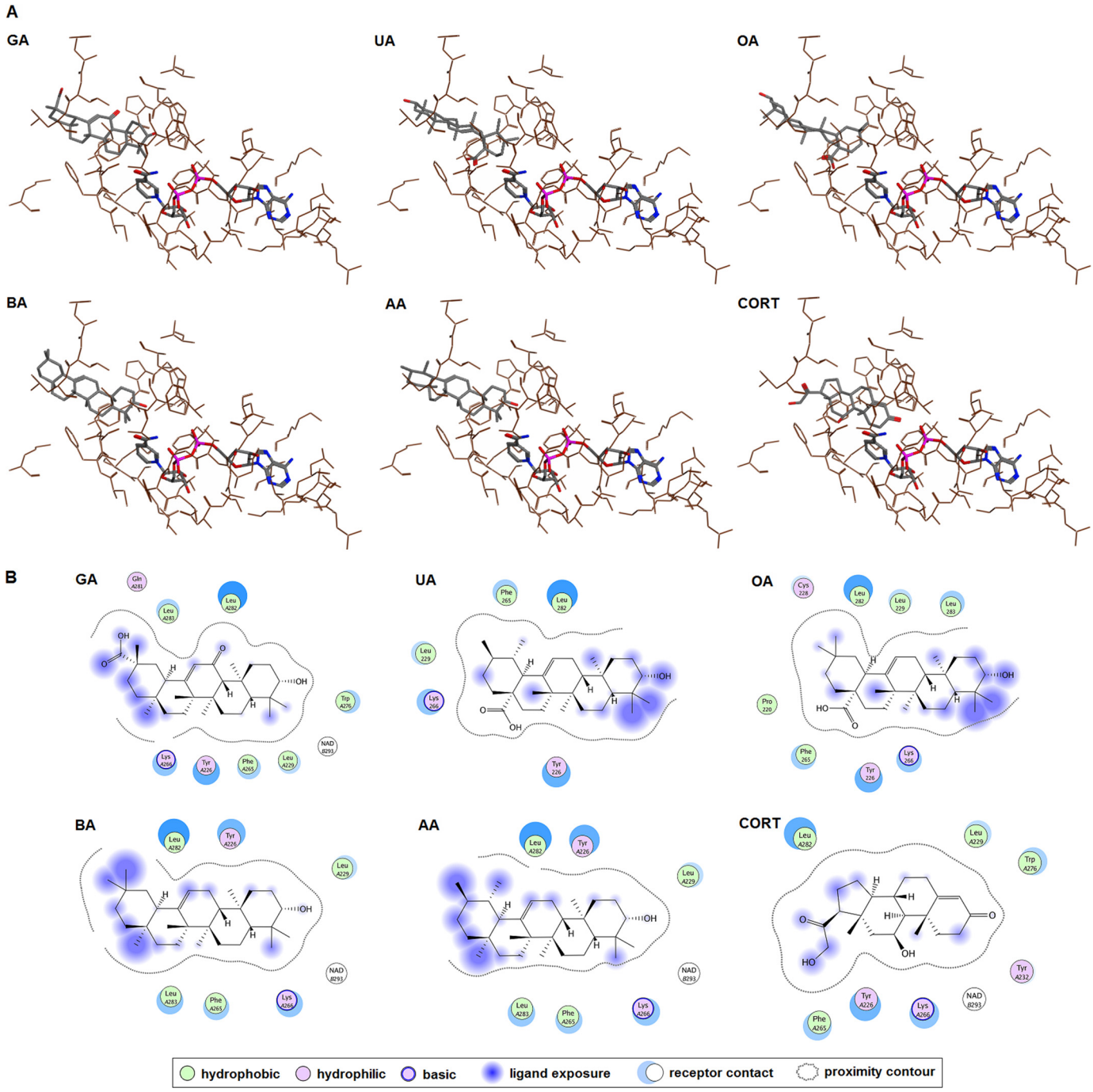

FIGURE 1. *A*, ASE-Dock findings between the triterpenoids and the 11βHSD2 model. The ASE-Dock module reveals that CORT, GA, UA, OA, BA, and AA exhibit similar binding orientations in the LBS in the 11βHSD2 model. The ligand fitting scores for GA, UA, AA, OA, and BA are −34.7, −28.6, −25.5, −24.8, and −24.7, respectively. The ASE scores for GA, OA, UA, AA, and BA are −12.0, −10.6, −6.8, 0.6, and 2.1, respectively. *Brown lines* are amino acid residues in the LBS. NAD^+ is also shown in each *panel*. *Blue*, nitrogen; *gray*, carbon; *purple*, phosphorus; and *red*, oxygen. *B*, ligand-receptor interaction between triterpenoids and 11βHSD2. The bound conformation of the triterpenoids in the LBS suggests the presence of hydrophobic interactions between GA and Leu-229, Phe-265, Trp-276, Leu-282, and Leu-283. UA has hydrophobic interactions with Leu-229, Phe-265, and Leu-282, and OA has hydrophobic interactions with Pro-220, Leu-229, Phe-265, Leu-282, and Leu-283. BA and AA also show some hydrophobic interactions with the residues in the LBS, but the hydrophobic and hydrophilic interactions are rather sporadic.

fibronectin (Biomedical Technologies, Cambridge, MA) in a humidified atmosphere containing 20% O_2 and 5% CO_2 at 37 °C.

Measurement of Antiproliferative Activity—Cells plated at 1×10^4 cells/well in 96-well microplates were treated with the test compounds at half confluency. After culture for another 24 h, the cell numbers were determined by the MTT assay (28).

Calculation of logP and PSA—The Spartan 06 program (Wavefunction, Inc., Irvine, CA) was adopted for calculation of logP from the Crippen model and PSA.

Western Blotting Analysis—Proteins were extracted with PBS containing 1 mM PMSF, 1 mM EDTA, 2 mM 2-mercaptoethanol, and 1% Triton X-100 at 4 °C for 3.5 h. For Western blotting analysis, aliquots of proteins were separated by SDS-PAGE,

Downloaded from www.jbc.org at MEIJO UNIVERSITY, on October 25, 2011

blotted onto a nitrocellulose membrane, and probed with a primary antibody followed by a secondary antibody. The primary antibodies used were mouse monoclonal anti-GAPDH (Santa Cruz Biotechnology, Santa Cruz, CA) and rabbit polyclonal anti-11βHSD2 (Cayman Chemical, Ann Arbor, MI). The secondary antibodies used were alkaline phosphatase-conjugated anti-mouse and anti-rabbit IgG_1 (Chemicon International, Temecula, CA). Visualization of the antigen-antibody complexes was performed with 33 μl of 5-bromo-4-chloro-3-indolyl phosphate, 66 μl of nitroblue tetrazolium, and 40 μl of 1 M $MgCl_2$ in 10 ml of 0.1 M Tris-HCl buffer (pH 9.5). Images of the positive bands were obtained by scanning, and the densities were determined using an LAS-3000 image analyzer (FujiFilm, Tokyo, Japan).

Time-lapse Microscopy—Cells plated on 60-mm diameter dishes were cultured with or without GA at half confluency in a mini incubator under a microscope (CK30; Olympus, Tokyo, Japan) and subjected to time-lapse microscopy using 10× and 20× objective lenses for 48–96 h (1 frame/10 min) and a digital imaging system equipped with a 3× magnification zoom-in camera (DIGA XP22V; Panasonic, Osaka, Japan).

Fluorescence Staining and Confocal Laser Scanning Microscopic Observation—Cells were fixed with 3.7% formaldehyde in PBS and permeabilized in PBS containing 0.1% Triton X-100. For F-actin labeling, cells were incubated with rhodamine-phalloidin. For βIII-tubulin labeling, cells were blocked in TBS containing 0.05% Tween 20 and 3% nonfat dried milk. Next, the cells were incubated with a mouse monoclonal anti-βIII-tubulin antibody (R&D Systems, Minneapolis, MN), washed with PBS, and incubated with HiLyte Fluor™ 488-conjugated goat anti-mouse IgG (AnaSpec, San Diego, CA). After washing and mounting with ProLong Gold anti-fade reagent (Molecular Probes, Eugene, OR), the cells were observed by confocal microscopy using an LSM510 META confocal laser scanning microscope equipped with Ar and He-Ne lasers (Carl Zeiss Japan, Tokyo, Japan) or a BIOREVO BZ-9000 fluorescence microscope system (Keyence, Osaka, Japan). Images were captured using 40× and 63× objective lenses, analyzed, and processed with the software Image Browser (Carl Zeiss Japan).

Measurement of CORT Levels—Inhibition of 11βHSD2 enzyme activity was assessed by measuring the increase in CORT accumulation in the culture medium supernatant. The 11βHSD2 enzyme activity inhibition was also examined in the reaction mixture reported by Mazzocchi *et al.* (29) except that CORT was used for the substrate and the reaction mixture contained 10 μM triterpenoids as inhibitors of 11βHSD2. The preparation of 11βHSD2 from the cells for the reaction mixture was prosecuted by the methods of Brown *et al.* (30), and samples were incubated at 37 °C for 1 h. The CORT levels were determined using a corticosterone enzyme immunoassay kit (Enzo Life Sciences International Inc., Plymouth Meeting, PA) in accordance with the manufacturer's protocol. The CORT levels were normalized to the cell numbers and expressed as ng/ml/10^6 cells.

Statistical Analysis—Experiments were performed in triplicate and repeated at least three times. The values quoted are given as means ± S.D. Ordinary or repeated-measures analysis of variance followed by Student's *t* test or Tukey-Kramer's multiple comparison test was used to evaluate the

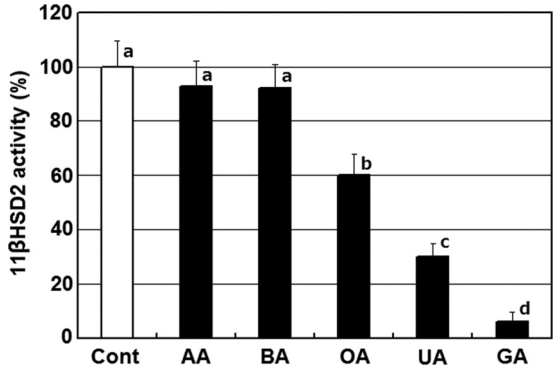

FIGURE 2. **11βHSD2 enzyme activity is inhibited by the triterpenoids.** 11βHSD2 was prepared by the methods of Brown *et al.* (30), and the samples were incubated in the reaction mixture reported by Mazzocchi *et al.* (29) in the presence of 10 μM each triterpenoid at 37 °C for 1 h. GA, UA, and OA significantly inhibit 11βHSD2 enzyme activity. Each point is the mean ± S.D. of three experiments. The *letter* for each treatment indicates a significant difference by Tukey-Kramer's test ($p < 0.05$).

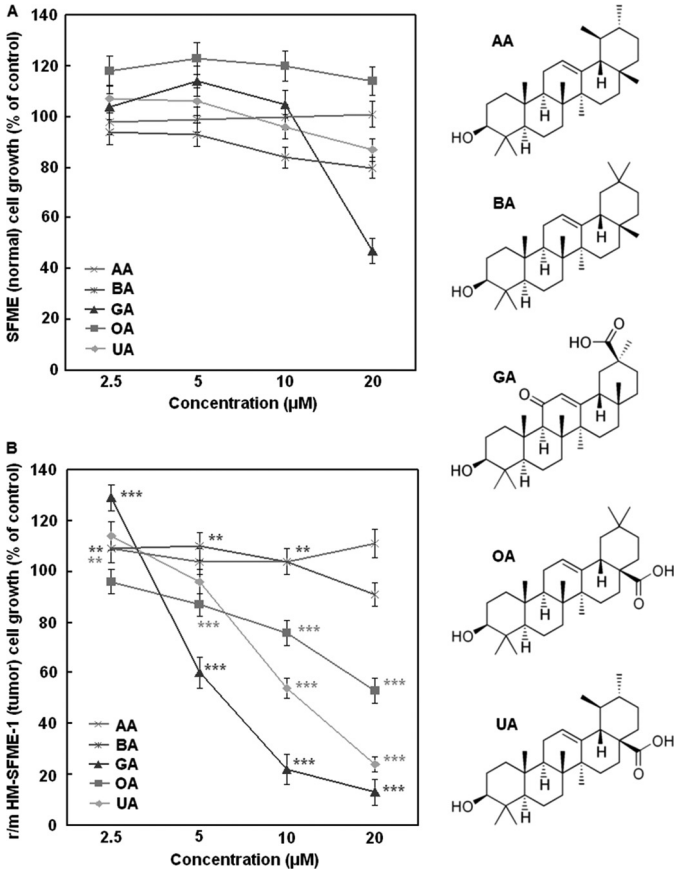

FIGURE 3. **GA is toxic to tumor cells without impeding normal cell growth.** Normal SFME and tumorigenic *r/m* HM-SFME-1 cells were treated with various concentrations of AA, BA, UA, OA, or GA for 24 h to investigate the effects on cell growth. *A*, >80% of the normal cells survive the 24-h triterpenoid treatments at concentrations of 2.5–10 μM, and GA treatment at 10 μM is not toxic to the cells at all. No statistical analysis was performed because there are no strong cytotoxic effects by the triterpenoid treatments at concentrations of 2.5–10 μM. *B*, GA inhibits ~80% of the tumor cells at 10 μM. Each point is the mean ± S.D. of at least three experiments. **, $p < 0.01$ and ***, $p < 0.001$ by Student's *t* test for normal cells *versus* tumor cells. The structures of the tested compounds are shown for reference.

Downloaded from www.jbc.org at MEIJO UNIVERSITY, on October 25, 2011

statistical significance of differences between groups. IC_{50} values were obtained using Prism 4.0 (GraphPad Software, Inc., San Diego, CA).

RESULTS

Ligand-Receptor Interaction between Triterpenoids and 11βHSD2—The ASE-Dock module revealed that, in addition to CORT (the substrate of 11βHSD2), GA, UA, OA, BA, and AA could bind to the LBS in the 11βHSD2 model and exhibited similar binding orientations (Fig. 1*A*). The ligand fitting scores for GA, UA, AA, OA, and BA were −34.7, −28.6, −25.5, −24.8, and −24.7, respectively. The ASE scores for GA, OA, UA, AA, and BA were −12.0, −10.6, −6.8, 0.6, and 2.1, respectively. Furthermore, to create ligand-receptor interaction plots for each triterpenoid-11βHSD2, the Ligand Interactions module of the Molecular Operating Environment 2009.10 was used, which provided a clearer arrangement of putative key intermolecular interactions that aid in interpretation of the three-dimensional juxtaposition of the ligands and the LBS in 11βHSD2 (Fig. 1*B*). Our results revealed the presence of hydrophobic interactions between GA and Leu-229, Phe-265, Trp-276, Leu-282, and Leu-283. UA had hydrophobic interactions with Leu-229, Phe-265, and Leu-282, and OA had hydrophobic interactions with Pro-220, Leu-229, Phe-265, Leu-282, and Leu-283. BA and AA also showed some hydrophobic interactions with the residues in the LBS, but the hydrophobic and hydrophilic interactions were rather sporadic, which may result in unstable binding of the ligands.

Effects of Triterpenoids on 11βHSD2 Enzyme Activity—The inhibition of 11βHSD2 enzyme activity was assessed by measuring the increase in CORT in the presence of 10 μM triterpenoids. GA, UA, and OA significantly inhibited 11βHSD2 enzyme activity (Fig. 2), which indicates that the tested triterpenoids bind to the enzyme at the catalytic site and have inhibitory effects on the enzymatic function. The inhibition rates for GA, UA, and OA were 94, 70, and 40%, respectively.

Antiproliferative Effects of Triterpenoids on Normal SFME and Tumorigenic r/m HM-SFME-1 Cells—The normal and tumor cells were treated with AA, BA, GA, OA, or UA at 2.5–20 μM for 24 h, and the effects on cell growth were examined. As shown in Fig. 3*A*, >80% of the normal cells survived the 24-h triterpenoid treatments at 2.5–10 μM, whereas GA treatment at 10 μM were not toxic to the cells at all. In contrast, ~20 and 50% of the proliferative capability of the tumor cells was inhibited by OA and UA at 10 μM, respectively, and GA was more potent, inhibiting ~80% of the tumor cell growth at 10 μM (Fig. 3*B*). The structures of the tested triterpenoids are also shown in Fig. 3 for reference.

Correlations between Cytotoxic Activity of Triterpenoids and Their logP and PSA Values—The mean 24-h IC_{50} values of the cells treated with AA, BA, GA, OA, or UA were determined, and the logP and PSA values of each triterpenoid were calculated (Table 1). Among the triterpenoids tested, GA, OA, and UA showed lower IC_{50} values for the tumor cells than for the normal cells. The difference in the IC_{50} values for GA between the normal cells and tumor cells was greater than those for OA or UA. Next, the IC_{50} values of the triterpenoids for the normal and tumor cells were analyzed with the logP and PSA values to examine whether there were correlations between them. The toxic activity of the tested triterpenoids against the normal cells showed no correlations with the logP and PSA values (Fig. 4, *A* and *C*). In contrast, the IC_{50} values for the tumor cells exhibited good correlations with the logP and PSA values (Fig. 4, *B* and *D*).

TABLE 1

Mean IC_{50} values of the cells treated with triterpenoids for 24 h and logP and PSA values of each triterpenoid

GA, OA, and UA show lower IC_{50} values for the tumor cells than for the normal cells. Each point is the mean ± S.D. of at least three experiments.

Triterpenoids	SFME cells	*r*/*m* HM-SFME-1 cells	logP	PSA
	μM	μM		A^2
AA	29.6 ± 4.9	46.2 ± 5.1[a]	8.26	18.59
BA	24.8 ± 3.2	37.5 ± 6.2[a]	8.40	18.58
GA	18.0 ± 4.0	7.3 ± 3.7[a]	7.11	64.02
OA	31.6 ± 6.3	21.0 ± 3.4[a]	7.47	51.72
UA	26.9 ± 5.1	11.2 ± 2.9[a]	7.33	51.76

[a] $p < 0.001$ by Student's *t* test for tumorigenic *r*/*m* HM-SFME-1 cells *versus* normal SFME cells.

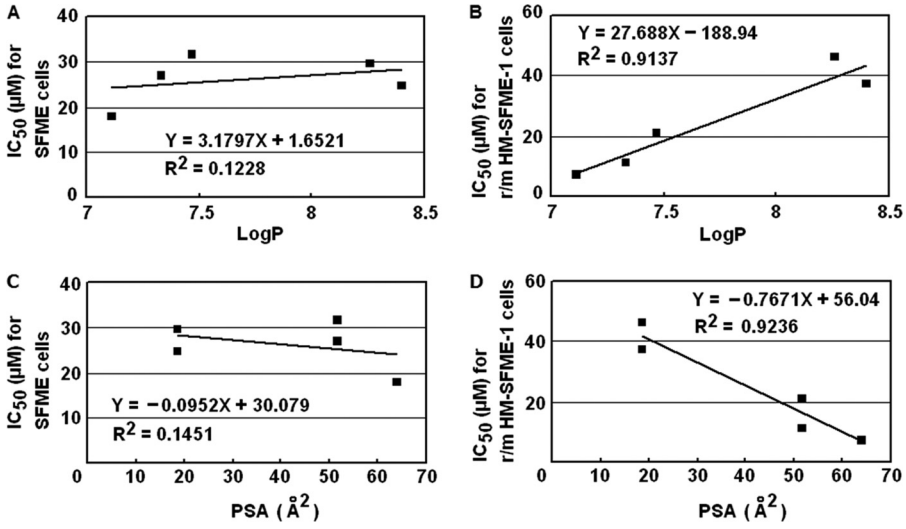

FIGURE 4. **Linear regression curves for the interaction of the logP and PSA values with the IC_{50} values of cell growth for SFME (*A* and *C*, respectively) and *r*/*m* HM-SFME-1 (*B* and *D*, respectively) cells.** Good direct (between the logP and IC_{50} values of each triterpenoid) and inverse (between the PSA and IC_{50} values of each triterpenoid) correlations are noted for the tumor cells. The individual values are shown in Table 1.

Downloaded from www.jbc.org at MEIJO UNIVERSITY, on October 25, 2011

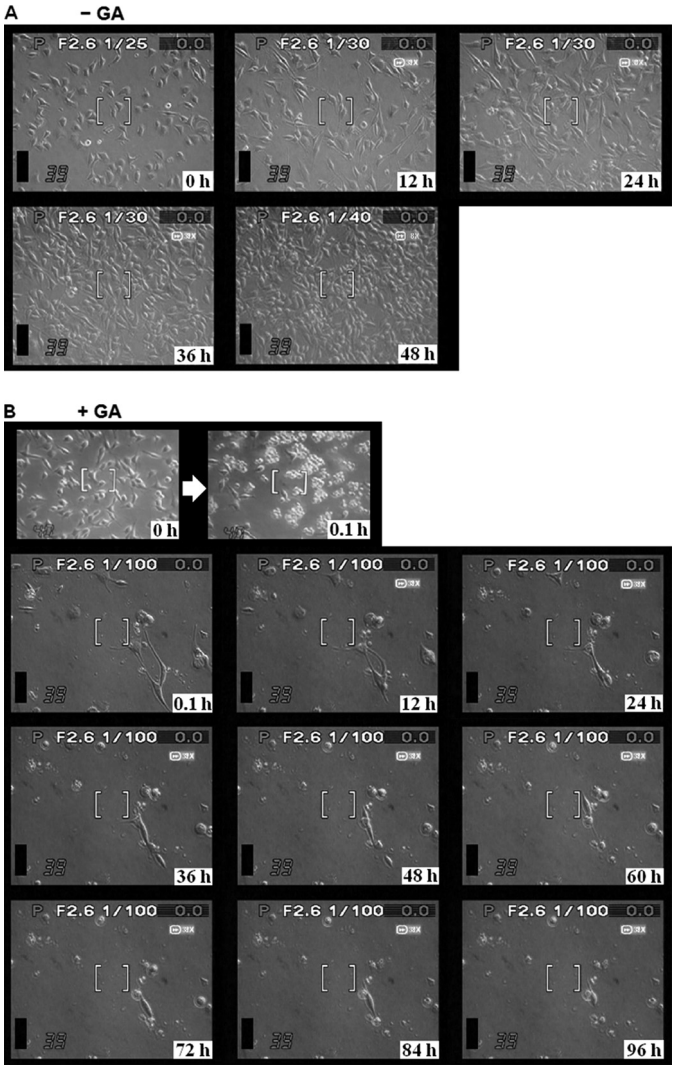

FIGURE 5. **GA can be toxic to the initially surviving tumor cells within 96 h.** Tumorigenic *r/m* HM-SFME-1 cells were treated with 10 μM GA and subjected to time-lapse microscopy for 96 h to determine whether the tumor cells could be affected after a long period of GA exposure. *A*, cells without GA treatment. *B*, the GA-treated tumor cells stop cell growth immediately and exhibit morphologic changes typical of apoptosis, such as cell shrinkage and blebbing. Cell toxicity seems to be induced in most of the cells within 96 h. The focus of the microscope is on the surviving cells (*0.1 h lower panel*), which are not surrounded by dead or floating cells and can still attach to the culture dish for 96 h even in the presence of GA, because the immediately affected dead or floating cells (*0.1 h upper panel*) make it hard to focus the microscope on the surviving cells.

Time-lapse Microscopy for GA-treated Tumor Cells—Thus far, we have analyzed the 24-h toxic effects of triterpenoids on tumor cell growth and found that GA was the most cytotoxic triterpenoid (Fig. 3*B* and Table 1). However, even at the very effective GA concentration of 10 μM for selective toxicity against the tumor cells, >15% of the tumor cells survived the 24-h treatment (Fig. 3*B*). If the GA exposure is prolonged, and the surviving tumor cells can gain resistance against GA and recover their growth and proliferative abilities, GA will lose its advantage as a selective antitumor agent. Therefore, we treated the tumor cells with 10 μM GA and performed time-lapse microscopy for 96 h to determine whether the tumor cells could still be affected after a long period of GA exposure. As shown in Fig. 5*A* and supplemental Movie S1, the tumor cells without GA treatment proliferated vigorously and reached confluency at 48 h. In contrast, the GA-treated tumor cells stopped cell growth immediately and exhibited morphologic changes typical of apoptosis, such as cell shrinkage and blebbing, and cell toxicity seemed to be induced in most of the cells within 96 h (Fig. 5*B* and supplemental Movie S2).

Effects of GA on Cytoskeletal Disruption—The GA-treated tumor cells exhibited cell shrinkage and blebbing (Fig. 5*B* and supplemental Movie S2), suggesting that GA could disrupt cytoskeletal proteins because they provide the cell shape and maintain the cellular structure (31). Therefore, the tumor cells were treated with GA at 10 μM for 24 h, and the effects on F-actin and βIII-tubulin in the cells were analyzed. As shown in Fig. 6 (*upper left Cont panel*), the tumor cells showed broad lamellipodia and F-actin extensions. In contrast, the GA-treated tumor cells exhibited disappearance of the F-actin extensions, and instead, staining was rather granulated and condensed (*upper right +GA panel*). The loss of F-actin extensions at the periphery of the cell membrane was particularly obvious, and the tumor cells were no longer capable of maintaining the characteristic broad lamellipodia. βIII-tubulin staining in the control cells (*middle left panel*) was homogeneous and mainly located in the cytoplasm, although its localization also extended into the broad lamellipodia. In contrast, the GA-treated cells showed non-homogeneous βIII-tubulin staining (*middle right panel* with an enlarged image), and voids or puncture-like disorganizations of βIII-tubulin were observed in the cytoplasm.

Effects of GA on 11βHSD2 Inhibition—Normal and tumor cells were treated with GA at 10 μM for 2, 8, and 24 h, and its effects on 11βHSD2 expression and the CORT levels were analyzed to assess the inhibition of 11βHSD2 enzyme activity. As shown in Fig. 7, *A* and *B*, endogenous 11βHSD2 expression was higher in the tumor cells, and this was also the case in the GA-treated tumor cells. The endogenous CORT level was also higher in the tumor cells, and GA treatment strongly elevated it further in a time-dependent manner (Fig. 7*C*).

DISCUSSION

For cancer prevention and therapy, selectivity is an important issue. An ideal antitumor agent should be toxic toward malignant cells, with minimum toxicity toward normal cells. However, there are currently only limited numbers of such agents available for clinical use (32). An example of such an agent is GLEEVEC, which targets the oncogenic breakpoint cluster region-abelson tyrosine kinase responsible for chronic myeloid leukemia (33). However, mutations and overexpression of the target molecules often lead to drug resistance, owing to multiple genetic and epigenetic alterations in tumor cells (34, 35). Moreover, tumor cells in advanced disease stages usually exhibit genetic instability and metabolic malfunction and are often resistant to conventional anticancer drugs (32). Therefore, with the intensive need for the development of more effective and safer agents for chemoprevention of cancer, natural products from plants, and their synthetic derivatives have been expected to be utilized in creating new and better chemopreventive and therapeutic agents (1). We previously reported that a naturally occurring triterpenoid, UA from apples, scarcely

Downloaded from www.jbc.org at MEIJO UNIVERSITY, on October 25, 2011

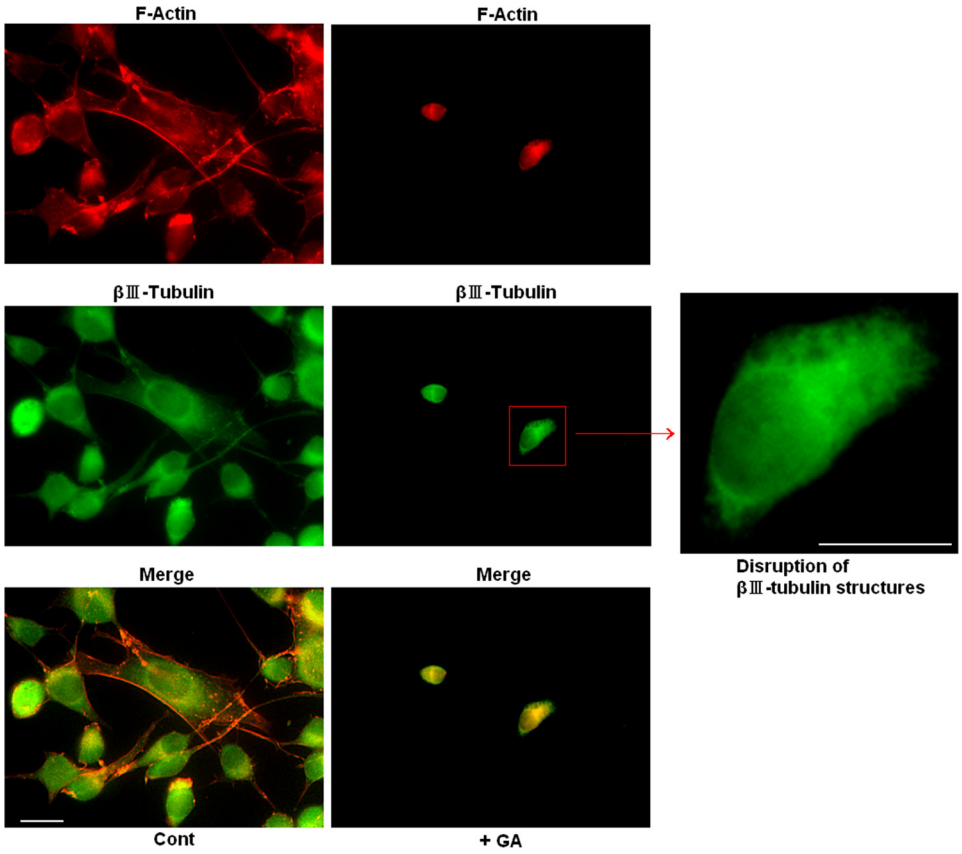

FIGURE 6. **GA disrupts cytoskeletal proteins.** Tumorigenic *r/m* HM-SFME-1 cells were treated with GA at 10 μM for 24 h, and its effects on F-actin and βIII-tubulin were analyzed. The tumor cells display broad lamellipodia and F-actin extensions (*upper left Cont panel*). In contrast, the GA-treated tumor cells exhibit disappearance of the F-actin extensions, and instead the staining is rather granulated and condensed (*upper right +GA panel*). Loss of the F-actin extensions at the periphery of the cell membrane is particularly obvious, and the tumor cells are no longer capable of maintaining the characteristic broad lamellipodia. In the *middle left panel*, βIII-tubulin staining in the control cells is homogeneous and mainly located in the cytoplasm but also extends into the broad lamellipodia. In contrast, in the *middle right panel*, the GA-treated cells show non-homogeneous βIII-tubulin staining, and voids or puncture-like disorganizations of βIII-tubulin are observed in the cytoplasm. *Scale bar*, 20 μm. An *enlarged image* of the *middle right panel* is also shown. *Scale bar*, 10 μm.

affected the viability of normal SFME cells, but markedly suppressed the growth of tumorigenic *r/m* HM-SFME-1 cells (2). Subsequently, we reported that another triterpenoid, GA from licorice, was not only selectively toxic to the tumor cells but also more potent than some clinically available antitumor agents in its selectivity (3). These abilities of UA and GA prompted us to investigate whether there were other potent triterpenoids that can inhibit tumor cell growth without hindering normal cell growth.

In the present study, the ASE-Dock module revealed that CORT (the substrate of 11βHSD2), GA, UA, OA, BA, and AA exhibited similar binding orientations in the LBS in the 11βHSD2 model, suggesting that triterpenoids can act as competitive inhibitors of CORT binding. The ligand fitting scores for the triterpenoid-11βHSD2 docking model revealed that the inhibitory effects of the triterpenoids on 11βHSD2 can be presumed in the order of GA > UA > AA ≈ OA ≈ BA. The ASE scores revealed that the inhibition against 11βHSD2 can be surmised in the order of GA > OA > UA > AA ≈ BA. Furthermore, the two-dimensional diagrams for the ligand-receptor interaction between the triterpenoids and 11βHSD2 showed that GA, UA, and OA would be more stably placed in the LBS than AA and BA. These *in silico* results suggest that 11βHSD2 can be inhibited by the triterpenoids in the order of GA > UA > OA > AA ≈ BA. The results for the inhibitory effects of the triterpenoids on 11βHSD2 enzyme activity also showed that 11βHSD2 can be inhibited by the triterpenoids in the order of GA > UA > OA > AA ≈ BA. In fact, our current *in vitro* results showed that GA, UA, and OA were selectively toxic against the tumor cells and that the selectivity of GA was more potent than any of the other triterpenoids tested. The selectivity of GA was such that, at 10 μM, it inhibited ~80% of the tumor cell growth within 24 h without affecting the normal cells and induced apoptosis in most of the tumor cells within 96 h. By analyzing the lipophilicity and toxic effects of some compounds from plants, Jiao *et al.* (36) reported that the logP values measured for some antitumor compounds were consistent with those predicted on the basis of their chemical structures and that logP values for measurement of the relative lipophilicity could be applied. Noshita *et al.* (37) reported good correlations between the PSA and the biological activities of an antitumor compound from wasabi (*Wasabia japonica*) and its synthetic derivatives. In the present study, we found that the IC_{50} values of the tested triterpenoids against the tumor cells showed a good direct and an inverse correlation with the logP and PSA values, respectively, suggesting that a certain degree of lower lipophilicity or higher PSA value is necessary for the toxic effects against the tumor cells. These findings also indicate

Downloaded from www.jbc.org at MEIJO UNIVERSITY, on October 25, 2011

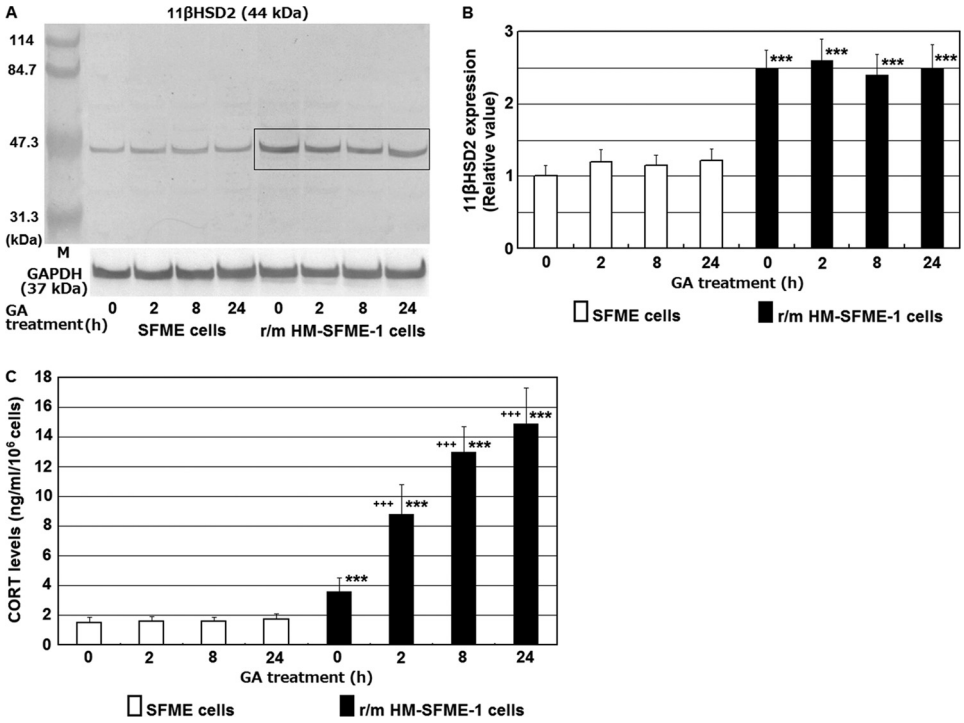

FIGURE 7. **11βHSD2 expression is higher in tumor cells than in normal cells, and GA up-regulates the CORT level in tumor cells.** Normal SFME and tumorigenic *r/m* HM-SFME-1 cells were treated with GA at 10 μM for 2, 8, and 24 h, and its effects on 11βHSD2 expression were analyzed. The CORT level was also analyzed to assess the inhibition of 11βHSD2 enzyme activity by GA. *A*, images of a Western blotting analysis. GAPDH was used as a loading control. *M*, Size markers. *B*, images of the Western blotting analysis were captured, analyzed, and processed with an image analyzer. As shown in the *rectangle* (*A*) and the *closed bars* (*B*), endogenous 11βHSD2 is higher in the tumor cells, and this is also the case in the GA-treated tumor cells. *C*, the endogenous CORT level is higher in the tumor cells, and the GA treatment elevates it further in a time-dependent manner. Each point is the mean ± S.D. of at least three experiments. ***, $p < 0.001$ by Student's *t* test for untreated normal cells *versus* untreated or treated tumor cells. +++, $p < 0.001$ by Student's *t* test for untreated tumor cells *versus* treated tumor cells.

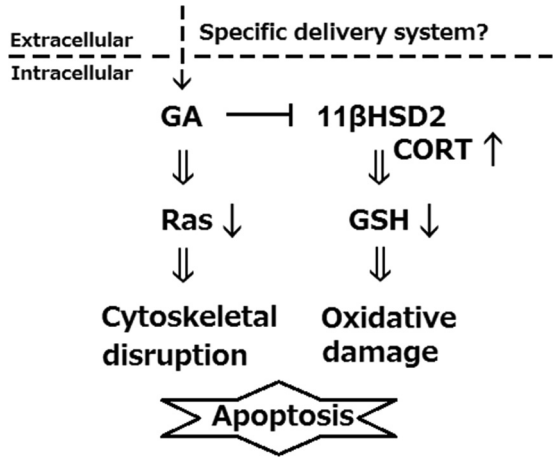

FIGURE 8. **Proposed mechanism underlying the 11βHSD2 inhibition by GA and tumor cell-selective toxicity.** GA is moved into the cells, possibly by a specific intracellular delivery system (Fig. 4, *B* and *D*). 11βHSD2 is overexpressed in various tumor cells (12–16), including the tumorigenic *r/m* HM-SFME-1 cells (Fig. 7, *A* and *B*). GA inhibits 11βHSD2 (Figs. 1, *A* and *B*, 2, and 7*C*; 13, 41), up-regulates CORT (Fig. 7*C*; 13), and down-regulates GSH (20). GA also down-regulates Ras (3). Decreased GSH and Ras make the cells vulnerable to oxidative damage (20) and cytoskeletal disruption (Fig. 6; 44, 45), which consequently lead to apoptosis of the tumor cells (Fig. 5*B* and supplemental Movie S2).

that a specific intracellular delivery system for triterpenoids may exist in the tumor cells.

Fig. 8 shows the proposed mechanism underlying the 11βHSD2 inhibition by GA and the tumor cell-selective toxicity. Our present results showed that the tumor cells exhibited higher 11βHSD2 expression, which suggests that the metabolic cascades through 11βHSD2 could be relatively easily triggered and that this may make the tumor cells sensitive to 11βHSD2 inhibition. It has been reported that patients with specific mutations in the 11βHSD2 gene developed severe CORT-dependent hypertension and other features of apparent mineralocorticoid excess (38). The other enzyme that could increase CORT is 11βHSD1. Increased 11βHSD1 and decreased 11βHSD2 expressions up-regulated CORT (39). 11βHSD1 acts as an oxoreductase converting 11-dehydrocorticosterone to CORT, whereas 11βHSD2 is a dehydrogenase that inactivates CORT (40), suggesting that increased activity of 11βHSD1 and/or decreased activity of 11βHSD2 up-regulate CORT. GA is a well known specific inhibitor of 11βHSD1 and 11βHSD2 (41). Furthermore, our current *in silico* and *in vitro* results revealed that 11βHSD2 could be inhibited and CORT was up-regulated by GA. Therefore, these reports and our present findings indicate that up-regulation of CORT is strongly associated with 11βHSD2 inhibition by GA. CORT is a known down-regulator of GSH (42), and inhibition of 11βHSD2 activity by GA up-regulated CORT and prevented tumor growth and metastasis (13), indicating that 11βHSD2 inhibition by GA induces down-regulation of GSH and consequently leads to suppression of tumor cell growth. This was exactly the case in our present and previous (20) studies, and the previous study also clearly revealed that the reactive oxygen species production levels were much higher, and the GSH levels were much lower in the tumor cells than in the normal cells. In the tumor cells,

Downloaded from www.jbc.org at MEIJO UNIVERSITY, on October 25, 2011

which produced higher reactive oxygen species levels and were already under oxidative stress, addition of GA, which would further elevate the production of reactive oxygen species, could lead to apoptosis of the tumor cells. Furthermore, the decrease in the GSH level by GA, which creates a redox imbalance, would lower the antioxidant capacity of the cells, which could contribute to death of the tumor cells. To the best of our knowledge, there have been no reports directly associating disruption of cytoskeletal proteins with 11βHSD2 inhibition by GA. Our current results could neither be interpreted as they have some association. Therefore, it remains unknown whether or not the disruption of the cytoskeletal proteins was a direct action of the 11βHSD2 inhibition. However, our previous study revealed the potential involvement of Ras in the selective toxicity by GA against the tumor cells (3). Ras pathways have been targeted for the development of chemotherapeutic interventions against tumor cells by interfering with cytoskeletal proteins such as actin (31) and tubulin (43). Furthermore, in our previous (44, 45) and current studies, we found that GA disrupted F-actin and βIII-tubulin, which could lead to loss of functionality for cell growth or proliferation and result in apoptosis of the cells. These findings indicate that disturbances in cytoskeletal proteins may be the factors involved in the toxic effects of GA against the tumor cells. It has been reported that interference with actin or microtubule functions associated with the integrity of the cytoskeleton could be utilized as a strategy for developing novel antitumor treatments (31). It has also been reported that some agents bind directly to cytoskeletal proteins, disrupt the integrity of tumor cells, and inhibit cell growth and proliferation (43, 46). Although further studies are required to elucidate whether the GA-mediated interference with the cytoskeletal proteins was a direct action or an indirect effect through some signaling pathways, our present study clearly reveals that disruption of cytoskeletal proteins could be one of the important factors that led to the induction of the selective tumor cell toxicity.

In conclusion, we utilized *in silico* analyses of the ligand-receptor interaction between triterpenoids and 11βHSD2 to predict the antitumor toxicity of some triterpenoids. The results of the *in silico* analyses were in good agreement with the *in vitro* experimental evidence. To the best of our knowledge, this is the first report on *in silico* prediction of the toxic effects of triterpenoids on tumor cells by 11βHSD2 inhibition. 11βHSD2 has been reported to be associated with various cancers and identified as a possible target for the prevention and therapy of cancer (12–16). In recent years, molecular modeling has gained much importance in the field of drug discovery and development (47–49), and further *in silico* studies of 11βHSD2 and its interactions with possible ligands are expected for the successful development of antitumor drugs targeting 11βHSD2.

REFERENCES

1. Martín, R., Carvalho-Tavares, J., Carvalho, J., Ibeas, E., Hernández, M., Ruiz-Gutierrez, V., and Nieto, M. L. (2007) *Cancer Res.* **67,** 3741–3751
2. Yamaguchi, H., Noshita, T., Kidachi, Y., Umetsu, H., Hayashi, M., Komiyama, K., Funayama, S., and Ryoyama, K. (2008) *J. Health Sci.* **54,** 654–660
3. Yu, T., Yamaguchi, H., Noshita, T., Kidachi, Y., Umetsu, H., and Ryoyama, K. (2010) *Toxicol. Lett.* **192,** 425–430
4. Loo, D. T., Fuquay, J. I., Rawson, C. L., and Barnes, D. W. (1987) *Science* **236,** 200–202
5. Loo, D., Rawson, C., Helmrich, A., and Barnes, D. (1989) *J. Cell Physiol.* **139,** 484–491
6. Rawson, C., Cosola-Smith, C., and Barnes, D. (1990) *Exp. Cell Res.* **186,** 177–181
7. Nomura, T., Matano, S., Okada, G., Tokuyama, H., Hori, I., Nakamura, S., Kameyama, T., and Ryoyama, K. (1993) *In Vitro Cell Dev. Biol.* **29A,** 614–616
8. Rawson, C., Shirahata, S., Collodi, P., Natsuno, T., and Barnes, D. (1991) *Oncogene* **6,** 487–489
9. Walker, B. R., Campbell, J. C., Williams, B. C., and Edwards, C. R. (1992) *Endocrinology* **131,** 970–972
10. Albiston, A. L., Obeyesekere, V. R., Smith, R. E., and Krozowski, Z. S. (1994) *Mol. Cell Endocrinol.* **105,** R11–17
11. Agarwal, A. K., Mune, T., Monder, C., and White, P. C. (1995) *Endocr. Res.* **21,** 389–397
12. Nigawara, T., Iwasaki, Y., Asai, M., Yoshida, M., Kambayashi, M., Sashinami, H., Hashimoto, K., and Suda, T. (2006) *Endocrinology* **147,** 769–772
13. Zhang, M. Z., Xu, J., Yao, B., Yin, H., Cai, Q., Shrubsole, M. J., Chen, X., Kon, V., Zheng, W., Pozzi, A., and Harris, R. C. (2009) *J. Clin. Invest.* **119,** 876–885
14. Koyama, K., Myles, K., Smith, R., and Krozowski, Z. (2001) *J. Steroid Biochem. Mol. Biol.* **76,** 153–159
15. Cohen, P. G. (2005) *Med. Hypotheses* **64,** 989–991
16. Zbánková, S., Bryndová, J., Kment, M., and Pácha, J. (2004) *Cancer Lett.* **210,** 95–100
17. Rabbitt, E. H., Lavery, G. G., Walker, E. A., Cooper, M. S., Stewart, P. M., and Hewison, M. (2002) *FASEB J.* **16,** 36–44
18. Stewart, P. M., and Prescott, S. M. (2009) *J. Clin. Invest.* **119,** 760–763
19. Rabbitt, E. H., Ayuk, J., Boelaert, K., Sheppard, M. C., Hewison, M., Stewart, P. M., and Gittoes, N. J. (2003) *Oncogene* **22,** 1663–1667
20. Yamaguchi, H., Yu, T., Kidachi, Y., Akitaya, T., Yoshida, K., Kamiie, K., Noshita, T., Umetsu, H., and Ryoyama, K. (2011) *Biochimie* **93,** 1172–1178
21. Levitt, M. (1992) *J. Mol. Biol.* **226,** 507–533
22. Fechteler, T., Dengler, U., and Schomburg, D. (1995) *J. Mol. Biol.* **253,** 114–131
23. Goto, J., Kataoka, R., Muta, H., and Hirayama, N. (2008) *J. Chem. Inf. Model.* **48,** 583–590
24. Hirakawa, H., Akita, H., Fujiwara, T., Sugai, M., and Kuhara, S. (2009) *Protein Eng. Des. Sel.* **22,** 385–391
25. Halgren, T. A. (1996) *J. Comput. Chem.* **17,** 490–519
26. Ham, R. G., and McKeehan, W. L. (1979) *Methods Enzymol.* **58,** 44–93
27. Mather, J. P., and Sato, G. H. (1979) *Exp. Cell Res.* **124,** 215–221
28. Carmichael, J., DeGraff, W. G., Gazdar, A. F., Minna, J. D., and Mitchell, J. B. (1987) *Cancer Res.* **47,** 943–946
29. Mazzocchi, G., Rossi, G. P., Neri, G., Malendowicz, L. K., Albertin, G., and Nussdorfer, G. G. (1998) *FASEB J.* **12,** 1533–1539
30. Brown, R. W., Chapman, K. E., Murad, P., Edwards, C. R., and Seckl, J. R. (1996) *Biochem. J.* **313,** 997–1005
31. Bijman, M. N., van Berkel, M. P., van Nieuw Amerongen, G. P., and Boven, E. (2008) *Biochem. Pharmacol.* **76,** 707–716
32. Trachootham, D., Zhou, Y., Zhang, H., Demizu, Y., Chen, Z., Pelicano, H., Chiao, P. J., Achanta, G., Arlinghaus, R. B., Liu, J., and Huang, P. (2006) *Cancer Cell* **10,** 241–252
33. Ren, R. (2005) *Nat. Rev. Cancer* **5,** 172–183
34. Couzin, J. (2002) *Science* **298,** 522–525
35. Frantz, S. (2005) *Nature* **437,** 942–943
36. Jiao, D., Eklind, K. I., Choi, C. I., Desai, D. H., Amin, S. G., and Chung, F. L. (1994) *Cancer Res.* **54,** 4327–4333
37. Noshita, T., Kidachi, Y., Funayama, H., Kiyota, H., Yamaguchi, H., and Ryoyama, K. (2009) *Eur. J. Med. Chem.* **44,** 4931–4936
38. Edwards, C. R., Benediktsson, R., Lindsay, R. S., and Seckl, J. R. (1996) *Steroids* **61,** 263–269

Downloaded from www.jbc.org at MEIJO UNIVERSITY, on October 25, 2011

39. Mark, P. J., Augustus, S., Lewis, J. L., Hewitt, D. P., and Waddell, B. J. (2009) *Biol. Reprod.* **80,** 1209–1215
40. Chapman, K. E., Gilmour, J. S., Coutinho, A. E., Savill, J. S., and Seckl, J. R. (2006) *Mol. Cell Endocrinol.* **248,** 3–8
41. Horigome, H., Horigome, A., Homma, M., Hirano, T., and Oka, K. (1999) *Am. J. Physiol. Endocrinol. Metab.* **277,** E624–630
42. Zafir, A., and Banu, N. (2009) *Stress* **12,** 167–177
43. Wasylyk, C., Zheng, H., Castell, C., Debussche, L., Multon, M. C., and Wasylyk, B. (2008) *Cancer Res.* **68,** 1275–1283
44. Yamaguchi, H., Kidachi, Y., Kamiie, K., Noshita, T., Umetsu, H., and Ryoyama, K. (2010) *Biol. Pharm. Bull.* **33,** 321–324
45. Yamaguchi, H., Noshita, T., Yu, T., Kidachi, Y., Kamiie, K., Umetsu, H., and Ryoyama, K. (2010) *Eur. J. Med. Chem.* **45,** 2943–2948
46. Tommasi, S., Mangia, A., Lacalamita, R., Bellizzi, A., Fedele, V., Chiriatti, A., Thomssen, C., Kendzierski, N., Latorre, A., Lorusso, V., Schittulli, F., Zito, F., Kavallaris, M., and Paradiso, A. (2007) *Int. J. Cancer* **120,** 2078–2085
47. Kurogi, Y., and Güner, O. F. (2001) *Curr. Med. Chem.* **8,** 1035–1055
48. Ekins, S. (2004) *Drug Discovery Today* **9,** 276–285
49. Jorgensen, W. L. (2004) *Science* **303,** 1813–1818

Downloaded from www.jbc.org at MEIJO UNIVERSITY, on October 25, 2011